Solar And Wind Powered Electric Auto Rickshaw Charging Optimization Using Giant Trevally Approach

J.E. Moshe Dayan * and A. Immanuel Selvakumar

Department of Electrical and Electronics Engineering, Karunya Institute of Technology and Sciences, Coimbatore 641114, Tamilnadu. India

* *Corresponding author. E-mail: reachmoshe@gmail.com*

Received: Apr. 25, 2026; Accepted: May. 16, 2026

Transportation is one of the main energy-related industries, and the energy sector has a major impact on the atmosphere and a large amount of global carbon pollution. The most popular mode of transportation for short-distance travel is the three-wheeler auto rickshaw, particularly when utilized as a taxi because of its compact design and minimal upkeep. But a plethora of trucks, buses, and rickshaws. These cars release a great deal of different poisonous and damaging particles and gases, and they require a lot of gasoline. This paper proposes a solar and wind-powered electric auto rickshaw. The proposed method is the Giant Trevally Optimizer (GTO). The objective of this proposed method is to reduce the total operation cost and emission of the system. The GTO method is utilized to provide an optimal solution by minimizing the cost of the system. By then, the performance of the proposed method is implemented in the MATLAB platform and compared to various existing techniques. The proposed method shows better results in all existing systems, like particle swarm optimization (PSO), artificial bee colony (ABC), and artificial neural network (ANN). In the proposed approach, the efficiency is 98%, which is higher than that of other existing systems.

Keywords: Electric Vehicle, Renewable Energy, Solar, Wind, Sickle Type Turbine

http://dx.doi.org/10.6180/jase.202611_34.059

1. Introduction

People are compelled by economic factors, environmental destruction caused by the use of fossil fuels, such as air pollution and global temperature rise [1]. Transportation accounts for 24% of global energy consumption, and in 2018, fossil fuel production provided a sizable portion of this need [2]. The use of traditional hydrocarbon fuels for transportation is crucial. Oil prices are below average, but this dependence leads to a host of issues, such as strain on finances and the stability of the energy supply [3]. Furthermore, the output of unconventional resources like shale oil is negligible; the world's fossil fuel reserves are depleting; and the environmental effects of these resources are becoming more pronounced. These factors have forced a radical shift in the energy sources, infrastructure, vehicles, and tools that rely on fossil fuels [4]. The techno-economic analysis of solar-powered EV charging systems for highlighting improved driving range and reliability in [5]. S. Singh et al. [6] proposed a gridconnected hybrid solar-wind system with EV charging support for a university shopping complex. K Prakash et al. [7] have suggested an energy-renewable hybrid electric vehicle (HEV) design, modeling, and control. To achieve the high torque requirements, the HEV design makes use of solar, wind, and fuel cells (FCs), which produce energy from proton exchange membranes (PEMs), as well as super capacitors (SCs). The car uses an FC as a backup energy source and a battery pack in addition to an SC to meet power requirements [8].

Recent research highlights the importance of solar- and wind-powered hybrid electric auto rickshaws for sustainable transportation and efficient battery energy management. Existing optimization techniques, such as ANN, PSO, and ABC, suffer from high cost and lower efficiency, motivating the development of the proposed Giant Trevally Optimizer (GTO)-based approach [9]. Electric vehicles (EVs), also known as green cars, still indirectly contribute to environmental pollution because conventional power grids rely on fossil fuels for electricity generation [10]. Therefore, integrating renewable energy sources (RES) such as solar and wind energy into EV transportation systems has become an important research focus. The development of "CleanCar" [11] and "Green-Car" technologies has gained significant attention worldwide for achieving sustainable and low-emission transportation. The contribution of the paper is as follows:

- Developed a 48V series-hybrid electric vehicle powered by a 2.2 HP Switched Reluctance Motor (SRM) with lightweight traction batteries.
- Integrated solar and wind energy support to enhance the vehicle driving range up to 72 km under zero-emission operation.
- Proposed and patented an intelligent hybrid energy management system where the petrol engine activates only at low battery SoC for efficient battery recharging.

The remaining portions of the document are arranged as follows: Section 2 describes the solar and wind-powered electric auto rickshaw, Section 3 describes the solar and wind-powered electric auto rickshaw using the GTO approach, Section 4 describes the results and discussion, and Section 5 completes the paper.

2. Configuration of solar and wind-powered electric auto rickshaw

The configuration of solar and wind-powered electric auto rickshaw is illustrated in Fig. 1. A switching reluctance motor (SRM) pushes the vehicle. The motor is powered by a lithium-ion battery pack and an EGS. The motor can be powered by both thermal and electric energy. The energy produced by the solar panel and wind turbine is stored in the battery. The generator transforms the engine's heat energy into electrical energy, which is then sent to the motor. The GTO method is utilized to provide an optimal solution by minimizing the cost of the system.

2.1. Savonius Wind Turbines

The cupped blades of the Savonius turbine harness wind energy to produce power. Generation is made feasible

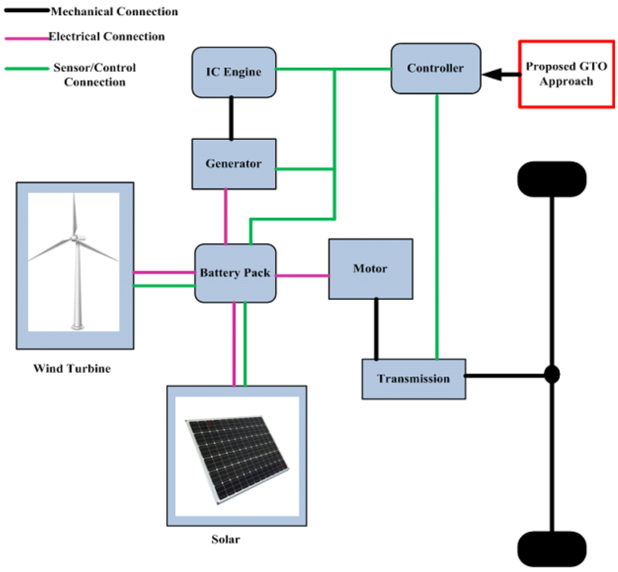

Fig. 1. Configuration of solar and wind powered electric auto rickshaw

by cupped blades, which have a higher drag coefficient while moving with the wind than when going against it. The difference between the torque applied to the generator's downwind and upwind blades is known as the let torque about the generator. A net positive torque is produced about the rotor center by an S-shaped Savonius turbine when positively contributed drag forces (FD +) exceed negatively contributed drag forces (FD). The Savonius turbine's power-generating capacity is determined by a number of significant parameters.

2.1.1. *Tip Speed Ratio (TSR)*

The speed of the tip: The ratio of a blade's tip speed to the distant wind velocity (v_0) is known as the definition of a ratio.

$$T.S.R = \lambda = R\omega / v_0 \tag{1}$$

2.1.2. *Cp Power Coefficient*

A turbine that produces power has efficiency if the swept area is defined as the area of the wind flow's cross section through which the turbine blade travels.

$$Cp = p / \left(1/2 \rho A_s v_0^3 \right) \tag{2}$$

ρ = Air density, typical savonius turbine = 0.12 to 0.15 at top speed ratio = 0.7. Nonetheless an optimized Savonius turbine theoretically $Cp = 0.32, T.S.R\lambda = 0.8$.

2.1.3. Start-Up Wind Velocity

The turbine spins at its lowest wind speed at this point. It depends greatly on the design and construction of the turbine, but it is usually in the range of a few meters per second.

2.1.4. Static Torque

It is the torque generated by the wind when the rotor is stationary around its center. The rotor angle frequently affects the static torque, and a high static torque frequently denotes a low wind speed at startup.

2.2. Sickle Type Turbine

The sickle-type turbine has the same theoretical calculation of dynamic performance as the Savonius turbine. This can be attributed to the larger curvature of the blade at the tip, increasing the tip speed ratio and hence the speed and hence the power delivered. From the experimental data that is obtained at time T = 30 s, the speed is 25 rpm without the addition of weight.

$$k_1 = v_b/v_q = R_\omega/v_0 = r_{25}/v_0 \tag{3}$$

When the 2 weights (approx. 300 g) are added at the tip,

$$k_2 = v_b/v_q = R_\omega/v_0 = r_{80}/v_0 \tag{4}$$

$$k_1/k_2 = 25/80 = 0.315 \tag{5}$$

$$k_2/k_1 = 3.2 \tag{6}$$

i.e., the k_2 with 2 tip weight is found to be 3.2 times the k_1 without tip weight.

$$\text{Hence,} \quad \lambda = k\left(1 + \frac{b}{2R}\right) \tag{7}$$

k s increased by 3.2 times, and the value is increased by 2.34 times.

$$\text{Therefore, } \lambda = 3.2k_1\,(2.3c_1) = 7.36c_1k_1 \tag{8}$$

$$\text{Normally to 2 (let's take 1.5) or 0.5} \tag{9}$$

$$\text{For, } k_1 = 0.3, \lambda = 0.3x_{2.3}x_{1.5}$$
$$\text{(ordinary Savonius turbine without weight)} \tag{10}$$

But in the model sickle, with the weights added

$$\lambda = 3.2\,(0.3x_{2.3}x_{1.5}) = 3.312 \tag{11}$$

Thus, the tip speed ratio is increased greater than 1, nearing the T.S.R Darrieus or horizontal axis turbine, which has T.S.R of 6. The problem of the low tip speed ratio of the vertical axis Savonius turbine, limited to 1, is solved by this model. Thus, our model of the turbine has the highest tip speed ratio.

2.3. Objective Function

In order to solve the intelligent distribution grid planning problem as effectively as feasible, the goal is to minimize both functions by taking constraints into account. These are the details of the multi-criteria optimization function.

$$\min\left\{L^{\cos t}, L^{\text{emission}}\right\} \tag{12}$$

The overall expenditure with $_{DG}$ is shown by function L. Two components make up this function. The costs associated with the fuselage and PV are covered in the first component, followed by the wind farm's operating costs in the second and the solar cell's operating costs in the third:

$$L = c_{wind(DG)} + c_{pv(DG)} \tag{13}$$

Function c_{PV} represents the $_{PV}$ function of the $_{DG}$,

The following formulas are used to determine exploitation costs for solar cells $c_{pv(DG)}$ and the cost of wind turbine exploitation, $c_{\text{wind }(DG)}$ respectively:

$$c_{\text{wind }(DG)} = \sum_{t=1}^{T}\sum_{\text{wind }=1}^{N_{\text{wind}}} \lambda_{\text{wind }(t)} \times P_{DG(\text{ wind },t)} \tag{14}$$

$$c_{PV}(DG) = \sum_{t=1}^{T}\sum_{pv=1}^{N_{PV}} \beta_{PV(t)} \times P_{DG(PV,t)} \tag{15}$$

The wind unit's power generation capacity is given by $P_{DG(\text{ wind },t)}$; the solar unit's generative energy is indicated by $P_{DG(PV,t)}$; and the exploitation cost coefficient of wind turbines is indicated by $\lambda_{\text{wind }(t)} \cdot \beta_{PV}$ serves as an indication of the wind solar cell cost efficiency. $P_{DG(PV,t)}$ stands for photovoltaic system-generated energy.

3. Proposed gto based solar and wind-powered electric auto rickshaw

The huge trevally is a member of the jack family and one of the biggest marine predators. The enormous kingfish is another term for it. They can also be found near the Hawaiian Islands and off the coast of East Africa. The behavior of the proposed GTO algorithm when pursuing seabirds is modeled after that of giant trevallies.

Step 1: initialization

Set up the input parameters, including current, power, and voltage.

Step 2: random generation

A random input parameter is produced in a matrix described by

$$Y = \begin{bmatrix} y_{1,1} & \cdots & y_{1,j} & \cdots & y_{1,d} \\ \vdots & \ddots & \vdots & \ddots & \vdots \\ y_{i,1} & \cdots & y_{i,j} & \cdots & y_{i,d} \\ \vdots & \ddots & \vdots & \ddots & \vdots \\ y_{n,1} & \cdots & y_{n,j} & \cdots & y_{n,d} \end{bmatrix} \quad (16)$$

Where, Y is denoted as the candidate solution of GTO, d is indicated as the quantity of decision variables in the given issue, n is represent as the quantity of members of GTO, d is indicated as the $y_{i,j}$ jth variable's value as indicated by the ith candidate solution.

Step 3: fitness calculation

To determine the fitness value using F

$$F = \text{Min}(L) \quad (17)$$

Where represents the overall cost

Step 4: exploration phase

The extensive search employing the Levy fly and the area selection process to identify the hunting region, which is provided below, reflects the exploration phase of the GTO.

A. levy flight to conduct an extensive search

To find food for the day, giant trevallies would travel great distances. Thus, in this stage, Eqn (18) is used to simulate the gigantic trevally's foraging movement patterns.

$$Y(T+1) = \text{best}_v \times r + ((\text{Max} - \text{Min}) \times r + \text{Min}) \times \text{Lévy}(d) \quad (18)$$

Where r is denoted as a number chosen at random that ranges from 0 to 1. best $_v$ is indicated as the area that gigantic trevallies are currently searching in, which they have chosen based on the best location from their previous search, $Y(T+1)$ is represent as the next iteration giant trevally position vector, and $\text{Leavy}(d)$ is indicated as the Levy flight is a distinct category of non-Gaussian stochastic processes, where the Levy distribution determines the step sizes. Random large steps help the algorithm's ability to search the entire globe. In this particular context, it is noteworthy since a multitude of studies have shown that a diverse array of species, particularly marine predators, exhibit Levy flying behavior. Leavy(d) can be calculated using Eqn (19),

$$\text{Leavy}(d) = \text{Step} \times \frac{U \times \sigma}{|A|^{1/\beta}} \quad (19)$$

Where U and A are indicated as random values in the interval $(0, 1)$ that are normally distributed, β is denoted as the flight distribution function's Levy index, it has a value range of 0 to 2 and is represented as the step size, set at a constant $0.01.\sigma$ is indicated as computed using Equation (20).

$$\sigma = \left(\frac{\Gamma(1+\beta) \times \sin e \left(\frac{\pi\beta}{2}\right)}{\Gamma\left(\frac{1+\beta}{2}\right) \times \beta \times 2^{\left(\frac{\beta-1}{2}\right)}} \right) \quad (20)$$

B. choosing an area step to identify the hunting region

In the choosing area step, gigantic trevallies locate and pick the optimal spot in the chosen search region for them to look for prey based on the quantity of food (seabirds). This phenomenon is mathematically simulated by Equation (21).

$$Y(T+1) = best_v \times b \times r + Mean\_Info - Y_i(T) \times r \quad (21)$$

Where, $Y(T+1)$ is denoted as the huge trevally's location vector in the subsequent iteration, T, b is indicated as the governing parameter for position change, which ranges from 0.3 to 0.4, $Y_i(T)$ is represent as the location of giant trevally at a time Mean_Info, refers to the mean, shows that the information from the preceding points has been fully utilized by these huge trevallies, and they can be computed using Equation (22).

$$\text{Mean\_Info} = \frac{1}{n} \sum_{i=1}^{n} Y_i(t) \quad (22)$$

Step 5: exploitation phase

Given below, the GTO's exploitation phase is exemplified by leaping out of the water to attack the prey:

A. attacking the prey by jumping out of the water

The medium through which the light beams are traveling is another crucial consideration.

Snell's Law uses refractive indices, which have set values for particular media, to demonstrate this relationship. Acting as an object, the bird is being observed by the large trevally.

Equation (23) below illustrates Snell's law.

$$\eta_1 \sin\theta_1 = \eta_2 \sin\theta_2 \quad (23)$$

Here, η_1 is the refractive index of air, η_2 is the refractive index of water, θ_1 and θ_2 represents the angle of refraction and incidence, θ_2 is the arbitrary value within the range (0 , 360).

From Eqn (23), θ_1 can be calculated using Eqn (24),

$$\sin\theta_1 = \frac{\eta_1}{\eta_2}\sin\theta_2 \tag{24}$$

Then, Eqn (25) can be used to compute the visual distortion.

$$A = \sin\left(\theta_1^{\circ}\right) \times D \tag{25}$$

Where D is indicated as the distance that can be calculated using Equation (26) between the attacker and the prey and is the variable's sine expressed in degrees.

$$D = \mid \left(\text{best}_{\,v} - Y_i(T) \right) \mid \tag{26}$$

Where, best $_v$ is the location of the prey and the best solution found thus far. Next, Equation (27) is used to develop a mathematical model of the behavior of gigantic trevally when they chase and leap out of the water.

$$Y(T+1) = L + A + H \tag{27}$$

Here, $Y(T+1)$ is denoted as the outcome of the following T iteration, which the attacking step generates, L is indicated as the launch speed to represent pursuing the bird.

Step 6: update the best solution

In each space, the algorithm explores new solutions, evaluates their fitness or quality, and updates the current solution if a better one is found.

Step 7: termination

Analyze the end criterion. if the best solution is identified, the process ends; if not, proceed to step 3.

4. Result and discussion

This sector provides an illustration of the proposed approach's performance based on the outcomes of the simulation. In this paper, a GTO method is utilized to provide optimal solution as minimizing cost of system. The proposed technique's performance is tested using the MATLAB working platform, and its results are contrasted with those of other currently used methods, such as PSO, ABC, and ANN.

Comparison of pollution reduction with proposed and existing method is illustrated in Fig. 2. In PSO approach the pollution reduction is 82%.

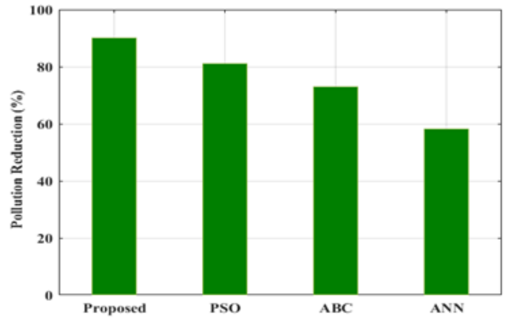

Fig. 2. Comparison of pollution with proposed and existing method

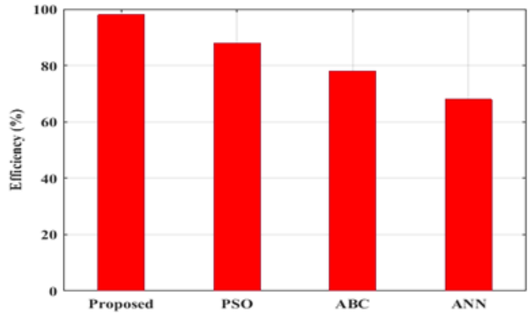

Fig. 3. Comparison of efficiency with the proposed and existing method

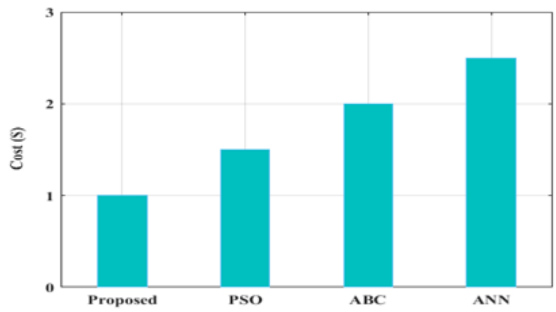

Fig. 4. Comparison of cost with proposed and existing method

Comparison of the sickle and savonius turbines is shown in Table 1. The savonius time is less than savonius voltage generator. The sickle-type time is less than the sticke-type voltage generator. The effect of various weights on the sickle turbine is shown in Table 2. Without weight the sickle turbine speed is 70RPM at 50 seconds. With a 2-tip weight, the sickle turbine speed is 80RPM at 50 sec. With a 4 tip weight the sickle turbine speed is 92RPM at 50 sec. The effect of centre deflector positioning without load is shown in Table 3. The no centre deflector, the speed is 77RPM at 36 sec. With the centre deflector, position 1, the

Table 1. Comparisons of sickle and Savonius turbines

Savonious (time in seconds)	Savonious (voltage generated)	Sickle type (time in seconds)	Sickle type (voltage generated)
40	10	5	2
60	45	25	53
140	63	50	64
200	71	150	90

Table 2. Effect of various weights on the sickle turbine

Without weight		With 2 Tip weight		With 4 tip weight	
Time (sec)	Speed (RPM)	Time (sec)	Speed (RPM)	Time (sec)	Speed (RPM)
10	10	10	20	10	30
18	18	18	56	12	65
30	25	30	81	30	86
50	70	50	89	50	92

Table 3. Effect of centre deflector positioning without load

No centre deflector		With centre deflector-shant position 1		With centre deflector-straight position		With centre deflector-shant position 2	
Time (sec)	Speed (RPM)	Time (sec)	Speed (RPM)	Time (sec)	Speed (RPM)	Time (sec)	Speed (RPM)
6	9.4	6	4	6	6	6	15
13	46	13	51	13	35	13	51
18	69	18	64	18	45	18	56
32	83	32	84	32	50	32	57

Table 4. Effect of centre deflector positioning with load

No centre deflector		With the centre deflector in the slant position		With the centre in a straight position	
Time (sec)	Speed (RPM)	Time (sec)	Speed (RPM)	Time (sec)	Speed (RPM)
39	12	5	12	10	12
70	21	7	21	15	21
100	33	17	30	17	23

Table 5. Analysis of cost

Rickshaw Type	Amount spend for petrol	Amount collected from passenger	Amount saved
Conventional auto rickshaw	500	900	400
Solar and wind-powered hybrid auto rickshaw	150	900	750

speed is 88RPM at 36 sec. With the centre deflector in the straight position, the speed is 56RPM at 36 sec . The with centre deflector shant position -2, the speed is 62RPM at 38 sec. The effect of centre deflector positioning with load is shown in Table 4. The no centre deflector, the speed is 33RPM at 100 sec. The centre deflector shant position the speed to 46RPM at 29 sec. With the centre deflector in the straight position, the speed is 36RPM at 57 sec. Analysis of cost is shown in Table 5. The solar and wind-powered hybrid auto rickshaw amounts saved more than the conventional rickshaw.

5. Conclusion

This work proposes a solar and wind-powered electric auto rickshaw using the GTO approach. Vehicles that use a lot of fuel and release a lot of different toxic, harmful particles and gases are affected by the proposed approach. The objective of this proposed method is to reduce the polluted emission and total operation cost of the system. In the MATLAB platform, the proposed approach is assessed and compared to other existing methods. All current systems, including artificial bee colonies (ABC), particle swarm optimization (PSO), and artificial neural networks (ANN), perform better when using the proposed method. The existing method of pollution reduction is 82%, 72%, 58%, and the proposed method of pollution reduction is 90%. The existing method efficiency is 88%, 78%, 68% and the proposed method efficiency is 98%. The existing method cost is 1.5$, 2$, 2.5$ and the proposed method efficiency is 1$. From the result, it is concluded that the proposed method shows high pollution reduction and high efficiency, and low cost compared to existing methods.

References

[1] M. Waseem, A. F. Sherwani, and M. Suhaib, (2019) *"Integration of Solar Energy in Electrical, Hybrid, Autonomous Vehicles: A Technological Review"* **SN Applied Sciences *1***: 1459. DOI: 10.1007/s42452-019-1458-4.

[2] S. D. Vidhya and M. Balaji, (2019) *"Modelling, Design and Control of a Light Electric Vehicle with Hybrid Energy Storage System for Indian Driving Cycle"* **Measurement and Control *52***: 1420–1433. DOI: 10.1177/0020294019858212.

[3] G. Mathesh and R. Saravanakumar, (2023) *"A Novel Digital Control Scheme for Power Management in a Hybrid Energy-Source Environment Pertaining to Electric Vehicle Applications"* **Frontiers in Energy Research *11***: 1130401. DOI: 10.3389/fenrg.2023.1130401.

[4] R. K. Majji, C. Bharatiraja, and S. Padmanaban, (2026) *"Grid-Integrated Solar PV Converter Operation Using Data-Driven Hybrid Control Approach"* **Results in Engineering *21***: 108814. DOI: 10.1016/j.rineng.2025.108814.

[5] G. Ramanathan, C. Bharatiraja, and J. L. Munda, (2024) *"PV-Assisted Grid-Connected Multi-Output Electric Vehicle Charger with PV2V, G2V and PV2G Functions"* **PLOS ONE *19***(6): e0304637. DOI: 10.1371/journal.pone.0304637.

[6] S. Singh, P. Chauhan, and N. J. Singh, (2021) *"Feasibility of a Grid-Connected Solar-Wind Hybrid System with an Electric Vehicle Charging Station"* **Journal of Modern Power Systems and Clean Energy *9***(2): 295–306. DOI: 10.35833/MPCE.2019.000387.

[7] K. Prakash, K. A. Mamun, F. R. Islam, A. A. Chand, K. A. Prasad, K. K. Goundar, and S. Maharaj. "Hybrid Electric Vehicle: Designing a Control of Solar/Wind/Battery/Capacitor/Fuel Cell Hybrid System". In: *Proceedings of the 29th Australasian Universities Power Engineering Conference (AUPEC)*. 2019, 1–6. DOI: 10.1109/AUPEC48475.2019.211000.

[8] F. Ahmad, M. Khalid, and B. K. Panigrahi, (2021) *"Development in Energy Storage System for Electric Transportation: A Comprehensive Review"* **Journal of Energy Storage *43***: 103153. DOI: 10.1016/j.est.2021.103153.

[9] A. K. Podder, S. A. Supti, S. Islam, M. Malvoni, A. Jayakumar, S. Deb, and N. M. Kumar, (2022) *"Feasibility Assessment of Hybrid Solar Photovoltaic-Biogas Generator Based Charging Station: A Case of Easy Bike and Auto Rickshaw Scenario in a Developing Nation"* **Sustainability *14***(1): 166. DOI: 10.3390/su14010166.

[10] P. Shrivastava, M. S. Alam, and M. S. J. Asghar, (2019) *"Design and Techno-Economic Analysis of Plug-In Electric Vehicle-Integrated Solar PV Charging System for India"* **IET Smart Grid 2**(2): 224–232. DOI: 10.1049/iet-stg.2018.0156.

[11] A. S. Ponrekha, M. S. P. Subathra, C. Bharatiraja, M. K. Nallapaneni, and H. H. Alhelou, (2025) *"A Topology Review and Comparative Analysis on Transformerless Grid-Connected Photovoltaic Inverters and Leakage Current Reduction Techniques"* **IET Renewable Power Generation *19***(1): e12655. DOI: 10.1049/rpg2.12655.